SCIENTIFIC REPORTS

OPEN

SUBJECT AREAS:
METALS AND ALLOYS
ATOMISTIC MODELS

Received
7 October 2014

Accepted
6 January 2015

Published
5 February 2015

Correspondence and requests for materials should be addressed to S.Y.W. (songyouwang@fudan.edu.cn) or C.Z.W. (wangcz@ameslab.gov)

Local structure order in $Pd_{78}Cu_6Si_{16}$ liquid

G. Q. Yue[1,2], Y. Zhang[2], Y. Sun[2], B. Shen[1], F. Dong[1], Z. Y. Wang[1], R. J. Zhang[1], Y. X. Zheng[1], M. J. Kramer[2], S. Y. Wang[1,2,3], C. Z. Wang[2], K. M. Ho[2] & L. Y. Chen[1]

[1]Shanghai Ultra-Precision Optical Manufacturing Engineering Center and Department of Optical Science and Engineering, Fudan University, Shanghai, 200433, China, [2]Ames Laboratory, U. S. Department of Energy and Department of Physics and Astronomy, Iowa State University, Ames, Iowa 50011, USA, [3]Key Laboratory for Information Science of Electromagnetic Waves (MoE), Shanghai 200433, China.

The short-range order (SRO) in $Pd_{78}Cu_6Si_{16}$ liquid was studied by high energy x-ray diffraction and *ab initio* molecular dynamics (MD) simulations. The calculated pair correlation functions at different temperatures agree well with the experimental results. The partial pair correlation functions from *ab intio* MD simulations indicate that Si atoms prefer to be uniformly distributed while Cu atoms tend to aggregate. By performing structure analysis using Honeycutt-Andersen index, Voronoi tessellation, and atomic cluster alignment method, we show that the icosahedron and face-centered cubic SRO increase upon cooling. The dominant SRO is the Pd-centered Pd_9Si_2 motif, namely the structure of which motif is similar to the structure of Pd-centered clusters in the Pd_9Si_2 crystal. The study further confirms the existence of trigonal prism capped with three half-octahedra that is reported as a structural unit in Pd-based amorphous alloys. The majority of Cu-centered clusters are icosahedra, suggesting that the presence of Cu is benefit to promote the glass forming ability.

Metallic glasses (MGs) containing the metalloid silicon constitute an important branch of glassy metals. The first MG prepared by rapid quenching was Au-Si[1]. These alloys had poor glass forming ability (GFA) and poor thermal stability relative to devitrification. Another group of Si-containing MGs are based on Pd-Si. Compared to Au-Si, Pd-Si has significantly enhanced GFA so that bulk metallic glasses (BMGs) can be readily prepared at the composition around $Pd_{80}Si_{20}$[2]. Meanwhile, Pd-Si BMGs possess intriguing mechanical properties[2]. Therefore Pd-based BMGs have drawn considerable research interests over the past decades. Early in 1972 Chen *et al*[3] found that the addition of Cu can significantly improve the thermal stability of Pd-Si MGs. As a result, the $Pd_{78}Cu_6Si_{16}$ MG, which lies close to the eutectic point of the ternary system has attracted interest due to a combination of excellent GFA, outstanding mechanical properties and promising hydrogen sensing ability[4–9].

Although the mechanical, thermal and dynamic properties have been studied experimentally[10–15], the atomic structures of $Pd_{78}Cu_6Si_{16}$ MG and its liquid still remain poorly understood. So far there are only several related reports about the structure of Pd-Si based glasses. Gaskell[16] is the first to propose that two types of trigonal prism structures are the probable candidates as a structure unit in Pd-Si MGs. One is a trigonal prism capped with three half-octahedra (9 Pd atoms around a Si atom), abbreviated as Si-9Pd and the other is a trigonal prism (6 Pd atoms around a Si atom). Then, Fukunaga et al.[17] further suggested that two types of trigonal prism structures may exist in $Pd_{85}Si_{15}$, $Pd_{80}Si_{20}$, and $Pd_{78}Si_{22}$ amorphous alloys through the analysis of the radial distribution function by neutron diffraction and geometrical structure relaxation simulations. However, radial distribution functions only provide a one-dimensional correlation of the structure and stoichiometry. In order to have a better understanding the structure in amorphous and liquid, higher-order correlations are necessary. Recently Kajita *et al*[18] found that Si content and Cu content have positive effect on the formation of a trigonal prism in Pd-based amorphous alloys. Nevertheless, the detailed atomic structure of liquid $Pd_{78}Cu_6Si_{16}$ and its evolution as well as the competition of multiple short range orders (SRO) upon cooling are still less understood.

In this paper, the structural property of liquid $Pd_{78}Cu_6Si_{16}$ is studied by high energy x-ray diffraction and *ab initio* MD simulations. To determine the special local structure in liquid $Pd_{78}Cu_6Si_{16}$ and analyze the development of the local structure with temperature, the total and partial pair-correlation functions (PCF), coordinate number (CN), Honeycutt and Andersen (HA) indices[19], Voronoi tessellation method[20] and atomistic cluster alignment (ACA) method[21] are used to analyze the trajectories from the *ab initio* MD simulations. It is revealed

that the dominant SRO around Si atoms is the trigonal prism capped with three half-octahedra (Si-9Pd) motif, while the majority of Cu-centered clusters are icosahedra, suggesting that the presence of Cu is benefit to promote the glass forming ability.

Results and Discussion

A. Pair correlation functions. As an important physical quantity to describe the structure of liquids, the PCF can be directly obtained by Fourier transform of experimental structure factor $S(q)$, which gives the possibility to find coordination atoms at a distance r from each central atom normalized by the average density. The PCFs of liquid $Pd_{78}Cu_6Si_{16}$ at different temperatures obtained from HEXRD experiment and *ab initio* MD simulations are presented in Fig. 1. All the PCFs exhibit typical features of metallic liquids, where a strong first peak centered at the average interatomic distance and a broadened second peak can be observed. It can be seen that the PCFs calculated by simulations are in good agreement with those from experiment, and the slight shift of calculated $g(r)$ to large direction of r may be caused by the density difference between the simulations and experiments. The first peaks become sharper upon cooling, indicating that the lower the temperature, the stronger the order of the system.

The partial PCFs (PPCFs) express the spatial correlations among different types of atoms. It is difficult to obtain PPCFs from experiment. However, PPCFs can be readily calculated in MD simulations. The PPCFs of liquid $Pd_{78}Cu_6Si_{16}$ are shown in Fig. 2. It is evident that the first peak of $g_{Pd\text{-}Si}(r)$ is the sharpest among all PPCFS, followed by $g_{Pd\text{-}cu}(r)$ and then $g_{Pd\text{-}Pd}(r)$, suggesting that the interaction between Pd-Si are stronger than Pd-Cu and Pd-Pd. And the height of these peaks increases in the process of quenching, contributing to the sharpening of the first peak in total PCFs. Meanwhile the peak position moves towards the smaller distance r as the temperature is decreased, reflecting densification of the system, consistent with the number density increasing mentioned later in Methods number density increasing. Despite its very low Cu and Si content, the sharp first peak of $g_{Cu\text{-}Cu}(r)$ indicates Cu atoms have a tendency to cluster. Nevertheless, the first peak of $g_{Si\text{-}Si}(r)$ is centered at about 4 Å, which is significantly larger than the length of direct Si-Si bond (2.35 Å). It demonstrates that there is no direct Si-Si bond within the first coordination shell in $Pd_{78}Cu_6Si_{16}$ liquids. The height of the first peak of $g_{Si\text{-}Cu}(r)$ tends to decrease while the height of the second peak tends to increase upon cooling, meaning that a repulsive interaction exists between Si and Cu atoms. Therefore the behaviors of Cu and Si atoms in liquid $Pd_{78}Cu_6Si_{16}$ are distinctly different, where Si atoms prefer to be separated from each other but Cu atoms tend to cluster together.

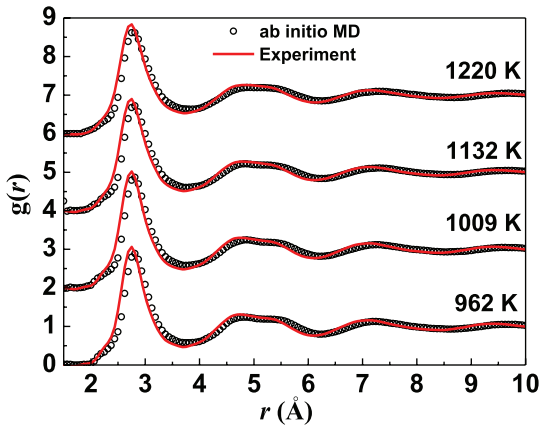

Figure 1 | Total pair correlation functions of liquid $Pd_{78}Cu_6Si_{16}$ at different temperatures.

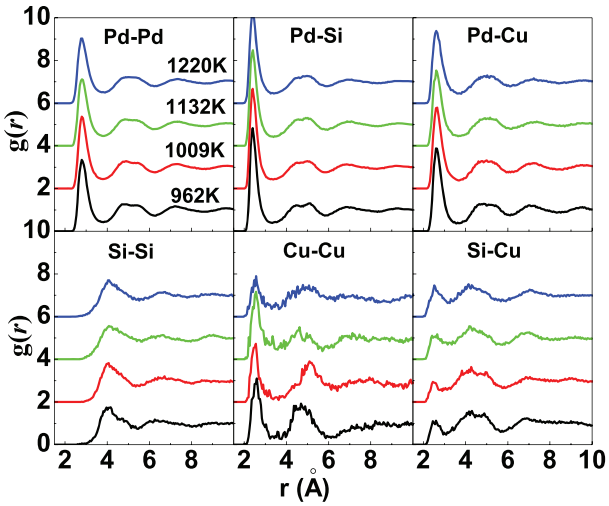

Figure 2 | Partial pair correlation functions of liquid $Pd_{78}Cu_6Si_{16}$ at different temperatures.

B. Short range order. According to the PPCFs described above, the coordination number (CN) can be obtained by integrating $g_{ij}(r)$ to the distance corresponding to first minimum in the $g_{ij}(r)$. The total and partial CNs are shown in Fig. 3. The total CN of Pd is the highest, followed by Cu and Si, which is mainly attributed to the largest atomic radius of Pd, then Cu and Si. The total CNs increase with the decrease of temperature, indicating the closer packing. The total CN of Cu is around 12. While the total CN around Si is about 9.5, which is in good agreement with the CNs of the trigonal prism capped with three half-octahedra structure in Ref. 17 From the partial CNs, it can be seen that the number of Si atoms around Cu is about 0.74~0.98, accounting for about 6.3~8.4% of total CN around Cu, far below the nominal Si content of 16%. Similar situation can be found for the CN of Si-Si. Consistent with the results discussed in the previous subsection that there exist repulsive interaction between Si-Cu and Si-Si.

The PCF and CN aforementioned describe the structure of the system only in one dimension. To obtain the three dimensional description of the SRO, the simplified HA-index method by Ganesh and Widom[22,23] is used to characterize the environment of each bond by counting the common neighbors surrounding the bond and indexing with a set of three numbers. The first number in HA-index will be 1 if the distance between the atomic pair is smaller than

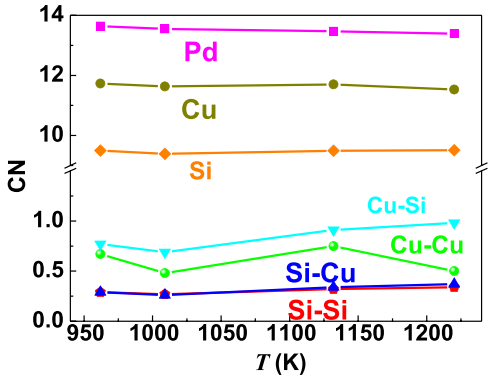

Figure 3 | CNs of liquid $Pd_{78}Cu_6Si_{16}$ at different temperatures. The three profiles from the top (labelled as Pd, Cu or Si) indicate the total CNs of Pd, Cu and Si atoms, respectively. The four curves at the bottom (labelled as A-B, where A is the central atom and B is the coordinated atom) are the partial CNs.

the r corresponding to the first minimum of g(r), indicating the atomic pair is bonded. Otherwise the first index will be 2. We will focus on the bonds with the first index of 1 in this work. The second index is the number of nearest neighbors shared by the atomic pair. The third index represents the number of bonds formed among the common nearest neighbors. Under this definition, the 155 index characterizes a part of perfect icosahedral (ICOS) local order, the 154 and 143 indices are characteristic of a part of distorted icosahedral (DICOS) ordering, the 142 index describes the face centered cubic (fcc) and hexagonal close-packed (hcp) ordering, the 166 and 144 indices are regarded as representative of body centered cubic (bcc) ordering, while the 131 and 132 indices represent other cubic order. The distribution of the HA index is shown in Fig. 4. It can be seen that the ICOS and DICOS are dominant with the fraction of about 60% with respect to the total number of bonds, while the sum of the 144 and 166 indices also occupies a higher proportion. Furthermore, the fraction of 155, 154, 143 and 142 indices increase, while the fraction of 144, 166, 131 and 132 change little as temperature drops. Overall, the SRO of the systems is enhanced with decreasing temperature, consistent with the results of $g(r)$, and the icosahedral ordering is the major part of the local structure all the time in the systems.

In order to describe the structure of clusters clearly, the Voronoi tessellation is used to further analyze the short range order in the liquids. The Voronoi polyhedrons (VPs) are enclosed by all the mid-perpendicular plane between the central atom and its neighbors, denoted by $<n_3, n_4, n_5, \ldots, n_i, \ldots>$ where n_i is the number of i-sided polygon. Fig. 5 gives the distribution of the top 17 representative clusters in the liquid $Pd_{78}Cu_6Si_{16}$. A cutoff distance of Rcut=5.0 Å is used in the Voronoi analysis. The VPs are divided into three groups, The first group is the Voronoi indices of the distorted fcc polyhedron <0,3,6,4,0>, <0,3,6,5,0>, <0,4,4,6,0>, and <0,4,4,7,0>. The second group is the Voronoi indices of the perfect ICOS <0,0,12,0,0> and DICOS <0,2,8,2,0> and <0,1,10,2,0>. The last group is other highly populated polyhedron. Among these various types of VPs, several VPs have a relatively high proportion and are strongly temperature-dependent, representing the evolution of the special order in the liquid. One can see that the percentage of the Voronoi indices of fcc-like and ICOS-like clusters is high and become higher with decreasing temperature, agreed with the results of HA index. While the fraction of the distorted icosahedral VPs <0,2,8,2> and <0,1,10,2> is higher than the perfect icosahedral VPs <0,0,12,0>. Although the fractions of bonds with the index of 155 is the highest in the HA analysis, formation of a perfect ICO requires twelve bonds with 155 indices, which is more difficult than formation of a DICOS with a combination of 155, 154 and 143 indices. Meanwhile, Voronoi tessellations reveal that fcc is competing with ICOS as the temperature is lowered. In the last group, one can see

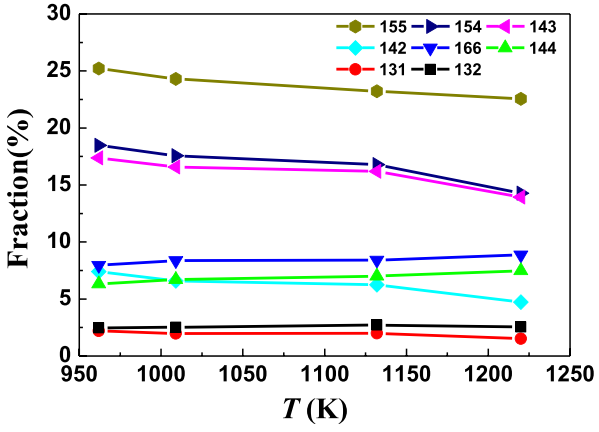

Figure 4 | The distribution of HA index for liquid $Pd_{78}Cu_6Si_{16}$ at different temperatures.

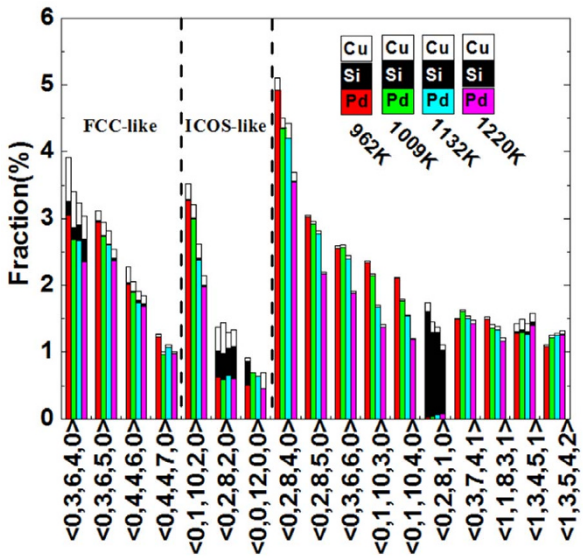

Figure 5 | The result of Voronoi tessellation analysis for liquid $Pd_{78}Cu_6Si_{16}$ at different temperatures.

clearly that Si-centered clusters prefer <0,2,8,1,0> VPs with lower CN while Pd-centered and Cu-centered clusters prefer other VPs of the higher CN, largely because the radius of Si atom is smaller than that of Pd and Cu atoms.

The cluster alignment method that describes the SRO and provides more insights into the average structure in the liquid and amorphous has recently been developed. This method has been shown to be able to give a direct visualization of the average local SRO[24,25] and medium range order[26,27]. In this paper, the SRO is analyzed by two types of alignment schemes. One is the collective cluster alignment, in which 2000 clusters with the same kind of central atoms were randomly selected from the MD simulation trajectories at each temperature. Each cluster is made up of 16 atoms. These clusters are then rigidly rotated and aligned to each other until the overall mean-square distances is minimized. Finally, the distributions of the atoms after the collective alignment are smoothed by a Gaussian smearing scheme to obtain three-dimensional atomic density distributions, which is the 3D representation of average SRO. The other alignment scheme is an individual cluster-template alignment. Each cluster in the system is aligned with a selected template to determine its structural similarity between the cluster and the tem-

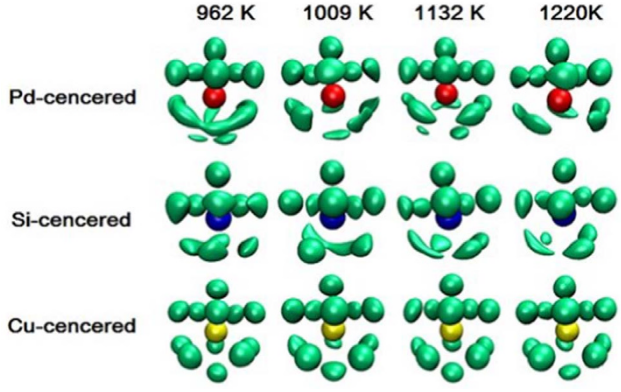

Figure 6 | The collective alignment results of liquid $Pd_{78}Cu_6Si_{16}$ at different temperatures. The upper panel stands for the Pd-centered (red) clusters. The middle panel describes the Si-centered (blue) clusters. The lower panel represents the Cu-centered (yellow) clusters. The isovalue is set to be 0.3 $Å^{-3}$.

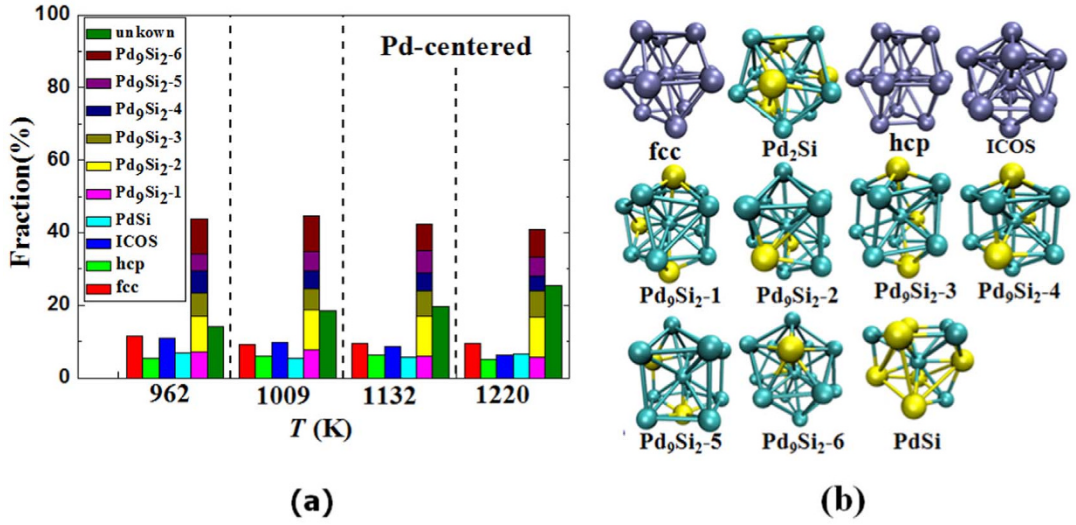

Figure 7 | (a) The fraction of different SRO in Pd-centered clusters (Pd_9Si_2-1, Pd_9Si_2-2, Pd_9Si_2-3, Pd_9Si_2-4, Pd_9Si_2-5, Pd_9Si_2-6 characterize all the distinct structures of Pd-centered clusters in Pd_9Si_2 crystal, PdSi represents the structure in Pd-centered clusters of PdSi crystal, and unknown indicate the structure which is not similar all the used templates. The nine types of Pd-centered clusters structure in Pd_2Si, Pd_3Si and Pd_5Si crystals and hcp with population less than 1% are not shown.). (b) the structures of fcc, hcp, ICOS and the main Pd-centered templates.

plate. Eventually, the population of each type of SRO can be obtained. For more details of cluster alignment method, we refer to Ref. 21.

The collective alignment results of liquid $Pd_{78}Cu_6Si_{16}$, centered by Pd atoms, Si atoms and Cu atoms respectively, are plotted in Fig. 6. The upper half parts of both Pd and Si centered patterns exhibit ICOS-like five-fold symmetry, while the lower half parts has no obvious symmetry. Unlike Pd and Si, the results of Cu centered patterns show the remarkable and complete ICOS-like symmetry.

To better understand the collective alignment results of liquid $Pd_{78}Cu_6Si_{16}$, the individual cluster-template alignment approach is used to quantify the different structure types. Sixteen types of Pd-centered and eight types of Si-centered clusters structure in Pd-Si binary Pd_2Si, Pd_3Si, Pd_5Si, Pd_9Si_2, and PdSi crystals which are all the crystals in the Pd-Si binary phase diagram[28] and whose crystal structures are illustrated in supplementary Fig. S3, and four types of the conventional SRO structure (bcc, fcc, hcp and ICOS) are used as templates in the alignment. The alignment results are shown in Fig. 7. Note that only 11 structure motifs are shown in Fig. 7, while those motifs with population less than 1% are not shown. If we align the templates among themselves, it was found that Pd-centered template of Pd_2Si is very similar to fcc. Hence this type of clusters is classified as fcc in the population plot. Among all the Pd-centered clusters of liquid $Pd_{78}Cu_6Si_{16}$, the Pd_9Si_2-like SRO are the most dominant, then ICOS and fcc, all of which increase with the drop of temperature, especially ICOS. This result can explain the collective alignment of Pd-centered clusters shown in Fig. 6 where the upper structures of Pd-centered clusters are similar to a fragment of ICOS, while there is no obvious symmetry in their lower structure.

The fraction of different SRO with the templates in Si-centered clusters and Cu-centered clusters are shown in Fig. 8. The structures of Si-centered clusters in Pd_2Si, Pd_3Si, and Pd_5Si crystals are very similar to a trigonal prism with three half octahedra (Si-9Pd), classified as Si-9Pd SRO. And two different Si-centered clusters structure in Pd_9Si_2 crystals are regarded as DICOS-1 and DICOS-2. It can be seen that Si-9Pd SRO accounts for about 60%, followed by DICOS about 30%, and the fraction of ICOS is less than 2%. These results are also consistent the collective alignment results for the Si-centered as shown in Fig. 6. For the Cu-centered clusters, the total fraction of DICOS and ICOS SRO in Fig. 8(c) is the highest, in accord with the collective alignment results shown in Fig. 6. However, there are also a substantial amount of Cu-centered clusters align well to the Si-centered template extracted from PdSi crystal, as one can see from Fig. 8 (c). This result suggests a part of Cu atoms may play a role of Si

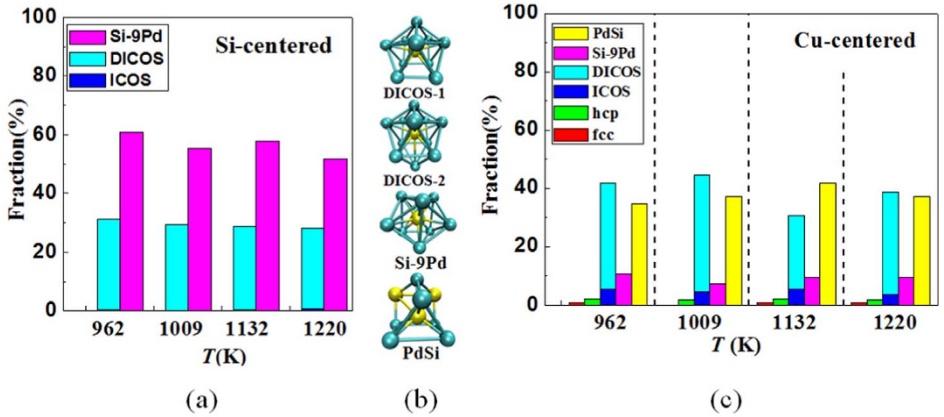

Figure 8 | (a) The fraction of different SRO in Si-centered clusters. (b) the structures of the main Si-centered templates. (c) The fraction of different SRO in Cu-centered clusters.

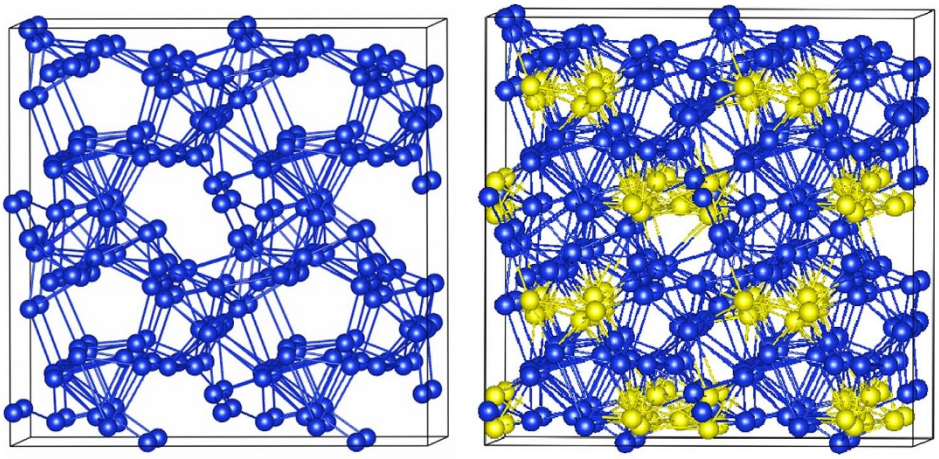

Figure 9 | (a) Si atoms network in liquid $Pd_{78}Cu_6Si_{16}$. (b) Si atoms and Cu atoms network in liquid $Pd_{78}Cu_6Si_{16}$. Periodic boundary conditions are used to extended the simulation box to a 2×2×2 cell in order to see the network more clearly. Si atom: blue, Cu atom: yellow.

atoms, forming the structure similar to that of Si-centered clusters in Pd-Si binary crystals.

From alignment results in Fig. 8 (a), it can be seen that the structures of Si-centered clusters are primarily Si-9Pd SRO and DICOS. Nearly half of Cu-centered clusters are also aligned well with the Si-centered PdSi template. Hence it would be very interesting to investigate the network formed by Si and Cu atoms in the $Pd_{78}Cu_6Si_{16}$ liquid. In Fig. 9 (a) and (b), the network formed by only Si atoms (blue) and formed by both Si and Cu atoms (yellow) in the liquid $Pd_{78}Cu_6Si_{16}$ at 962 K are shown, respectively. The distance between Si atoms are almost more than 4 Å, much larger than the Si-Si bond length, consistent with the PCF and CN results discussed above. Compared Fig. 9 (a) with (b), It can be clearly seen that the Si-only network contains some voids, Cu atoms tend to form small clusters and fill the voids in the Si atoms network as one can see from Fig. 9(b). Although the medium order among Si atoms is not obvious, there are a lot of the isosceles triangles in the Si network.

Conclusions

In summary, the local structure of liquid $Pd_{78}Cu_6Si_{16}$ was studied by *ab initio* MD simulations and high energy x-ray diffraction. The calculated PCFs at different temperatures agreed well with the experiments. The analysis of the PPCFs indicates that Si atoms prefer to be separated from each other and form network while Cu atoms tend to form small cluster to fill the holes in the Si atom network. The results of the density and CNs show that the system is more close-packed with decreasing temperature. HA-index, Voronoi tessellation, and ACA method provide a detailed 3D description of the local atomic structures in the liquid. It is found that ICOS and fcc order increase with decreasing temperature. The dominant polyhedral order is Pd-centered clusters structure in the motif of Pd_9Si_2 crystals, and Si-9Pd SRO of Si-centered clusters observed on experiment[17]. In Cu-centered clusters, there is a high proportion of DICOS and ICOS SRO, suggesting that the presence of Cu is benefit to the formation of glass.

Methods

Experiments. $Pd_{78}Cu_6Si_{16}$ alloys were prepared by arc melting the mixtures of pure Pd (99.99%), Si (99.99%) and Cu (99.99%) in an ultra-high-purity argon atmosphere. Next, the ingot was wrapped in Ta foil, sealed in quartz tubes backfilled with Ar. After annealed at $0.9T_m$ (the melting temperature of the sample is 1033 K) for 24 hours, the tube was quenched in water. The high energy X-ray diffraction (HEXRD) was performed at the Advanced Photon Source (APS) of the Argonne National Laboratory (DuPage County, IL), using an energy of 99.55 keV, which corresponded to a wavelength (λ) of 0.0124(7) nm. The diffraction data were collected at the 6ID-D beamline at APS. Silicon double-crystal monochromators were employed to select the wavelength. The HEXRD was obtained in a time-resolved manner using a charge-coupled device (CCD, MAR Research, Evanston, IL) detector in an off-beam-axis mode, in which only a 60-deg arc of the Debye cones intersected the CCD. The sample-to-detector distance was calibrated using a National Institute of Standards and Technology (NIST) Si (640C) standard. Then the intensity data were converted to the total structure factor $S(q)$ using PDFGetX2 with appropriate container and background subtractions and the reduced correlation function $g(r)$ by Fourier transform.

Simulations. The *ab initio* MD simulations were carried out using the Vienna *ab initio* simulation package (VASP) code based on the density functional theory[29,30], with the projector-augmented wave method[31,32] and the Perdew-Burke-Ernzerhof generalized gradient approximation. A canonical ensemble with Nosé-Hoover thermostat to control the temperature was used[33,34]. The time step was set to be 3 fs. A cubic cell containing 200 atoms (156 Pd, 32 Si and 12 Cu atoms) with random distribution was taken as the initial configuration. Periodic boundary conditions were applied throughout the simulation. Only the Γ point was used to sample the Brillouin zone of the supercell. Firstly, the initial configuration was heated to a high temperature well above the melting point of 1033 K, so as to eliminate any memory effect from the initial configuration. Then the liquid was cooled down to 1220, 1132, 1009, and 962 K at a constant cooling rate of 0.1 K/step, respectively. At each temperature, the average pressure of the system was adjusted to 0.0 ± 1.0 kB by changing the dimensions of the simulation box. The optimized number densities were 0.0632, 0.0629, 0.0624, and 0.0620 atom/Å^3 at 962, 1009, 1132 and 1220 K, respectively. From the change in the diffusion coefficient, it can be seen that the $Pd_{78}Cu_6Si_{16}$ alloy at 962 K and 1009 K are in the undercooled liquid state, as illustrated in supplementary Fig. S1. In order to study the structural and dynamical properties of the liquid, additional 4000 time steps were performed at each temperature and the atomic trajectories were collected.

1. Klement, W., Willens, R. H. & Duwez, P. Non-crystalline structure in solidified Gold-Silicon alloys. *Nature* **187**, 869–870 (1960).
2. Yao, K. F., Ruan, F., Yang, Y. Q. & Chen, N. Superductile bulk metallic glass. *Appl. Phys. Lett.* **88**, 122106 (2006).
3. Chen, H. S. & Park, B. K. Role of chemical bonding in metallic glasses. *Acta Metall.* **21**, 395–400 (1973).
4. Bøttiger, J., Dyrbye, K., Pampus, K., Torp, B. & Wiene, P. H. Tracer diffusion in amorphous Pd-Cu-Si. *Phys. Rev. B* **37**, 9951–9954 (1988).
5. Dyrbye, K., Bøttiger, J., Pampus, K. & Torp, B. Radiation-enhanced diffusion in amorphous Pd-Cu-Si. *Phys. Rev. B* **38**, 8562–8565 (1988).
6. Schwabe, M., Kuchemann, S., Wagner, H., Bedorf, D. & Samwer, K. Activation volume of microscopic processes in amorphous $Pd_{77.5}Cu_{6.0}Si_{16.5}$ due to stress and temperature. *J. Non-Cryst. Solids* **357**, 490–493 (2011).
7. Steinberg, J., Tyagi, S. & Lord, A. E. Calculation of the critical cooling rate for amorphous $Pd_{77.5}Si_{16.5}Cu_6$. *Appl. Phys. Lett.* **38**, 878–880 (1981).
8. Kajita, S., Kohara, S., Onodera, Y., Fukunaga, T. & Matsubara, E. Effect of Composition and Microstructure of Pd-Cu-Si Metallic Glassy Alloy Thin Films on Hydrogen Absorbing Properties. *Mater. Trans.* **52**, 1807–1813 (2011).
9. Kajita, S., Yamaura, S., Kimura, H. & Inoue, A. Hydrogen sensing ability of Pd-based amorphous alloys. *Sens. Actuators B* **150**, 279–284 (2010).
10. Yao, K. F., Yang, Y. Q. & Chen, N. Mechanical properties of Pd–Cu–Si bulk metallic glass. *Intermetallics* **15**, 639–643 (2007).

11. Wilde, G., Lu, I. R. & Willnecker, R. Fragility, thermodynamic properties, and thermal stability of Pd-rich glass forming liquids. *Mater. Sci. Eng. A* **375–377**, 417–421 (2004).
12. Fiore, G. & Battezzati, L. Thermodynamic properties of the $Pd_{77.5}Cu_6Si_{16.5}$ undercooled liquid. *J. Alloys and Comp.* **483**, 54–56 (2009).
13. Esquinazi, P., König, R. & Pobell, F. Acoustic properties of amorphous SiO_2 and PdSiCu, and of crystalline Ag, NbTi and Ta at very low temperatures. *Z. Physik B - Condensed Matter* **87**, 305–321 (1992).
14. Egry, I., Lohöfer, G., Seyhan, I., Schneider, S. & Feuerbacher, B. Viscosity of eutectic $Pd_{78}Cu_6Si_{16}$ measured by the oscillating drop technique in microgravity. *Appl. Phys. Lett.* **73**, 462–463 (1998).
15. Chen, H. S. & Goldstein, M. Anomalous viscoelastic behavior of metallic glasses of Pd-Si based alloys. *J. Appl. Phys.* **43**, 1642–1648 (1972).
16. Gaskell, P. H. A new structural model for amorphous transition metal silicides, borides, phosphides and carbides. *J. Non-Cryst. Solids* **32**, 207–224 (1979).
17. Fukunaga, T. & Suzuki, K. Radial Distribution Functions of Pd-Si Alloy Glasses by Pulsed Neutron Total Scattering Measurements and Geometrical Structure Relaxation Simulations. *Sci. Rep. Res. Inst. Tohoku Univ.* **29**, 153–175 (1980).
18. Kajita, S., Kohara, S., Onodera, Y., Fukunaga, T. & Matsubara, E. Structural Analysis of Pd-Cu-Si Metallic Glassy Alloy Thin Films with Varying Glass Transition Temperature. *Mater. Trans.* **52**, 1349–1355 (2011).
19. Honeycutt, J. D. & Andersen, H. C. Molecular-dynamics study of melting and freezing of small Lennard-Jones clusters. *J. Phys. Chem.* **91**, 4950–4963 (1987).
20. Finney, J. Modelling the structures of amorphous metals and alloys. *Nature* **266**, 309–314 (1977).
21. Fang, X. W., Wang, C. Z., Yao, Y. X., Ding, Z. J. & Ho, K. M. Atomistic cluster alignment method for local order mining in liquids and glasses. *Phys. Rev. B* **82**, 184204 (2010).
22. Ganesh, P. & Widom, M. Signature of nearly icosahedral structures in liquid and supercooled liquid copper. *Phys. Rev. B* **74**, 134205 (2006).
23. Ganesh, P. & Widom, M. Ab initio simulations of geometrical frustration in supercooled liquid Fe and Fe-based metallic glass. *Phys. Rev. B* **77**, 014205 (2008).
24. Shen, B. *et al.* Molecular dynamics simulation studies of structural and dynamical properties of rapidly quenched Al. *J. Non-Cryst. Solids* **383**, 13–20 (2014).
25. Wu, S. *et al.* Structural and dynamical properties of liquid $Cu_{80}Si_{20}$ alloy studied experimentally and by ab initio molecular dynamics simulations. *Phys. Rev. B* **84**, 134208 (2011).
26. Fang, X. W. *et al.* Spatially Resolved Distribution Function and the Medium-Range Order in Metallic Liquid and Glass. *Sci. Rep.* **1**, 194 (2011).
27. Ke, F. S. *et al.* Bergman-type Medium-Range Order in Rapid Quenched $Ag_{0.74}Ge_{0.26}$ Eutectic Alloy studied by ab initio Molecular Dynamics. *Acta Mater.* **80**, 498–504 (2014).
28. Baxi, H. C. & Massalski, T. B. The PdSi (palladium silicon) system. *J. Phase Equilib.* **12**, 349–356 (1991).
29. Kresse, G. & Hafner, J. Ab initio molecular dynamics for liquid metals. *Phys. Rev. B* **47**, 558–561 (1993).
30. Kresse, G. & Furthmuller, J. Efficiency of ab-initio total energy calculations for metals and semiconductors using a plane-wave basis set. *Comput. Mater. Sci.* **6**, 15–50 (1996).
31. Blochl, P. E. Projector augmented-wave method. *Phys. Rev. B* **50**, 17953–17979 (1994).
32. Kresse, G. & Joubert, D. From ultrasoft pseudopotentials to the projector augmented-wave method. *Phys. Rev. B* **59**, 1758–1775 (1999).
33. Nose, S. A unified formulation of the constant temperature molecular dynamics methods. *J. Chem. Phys.* **81**, 511–519 (1984).
34. Hoover, W. G. Canonical dynamics: Equilibrium phase-space distributions. *Phys. Rev. A* **31**, 1695–1697 (1985).

Acknowledgments

The work at Fudan university was supported by the NSF of China (Grant Nos. 11374055 and 10974029), National Basic Research Program of China (Nos. 2010CB933703 and 2012CB934303), and the Fudan High-end Computing Center. Work at Ames Laboratory was supported by the US Department of Energy, Basic Energy Sciences, and Division of Materials Science and Engineering, including a grant of computer time at the National Energy Research Scientific Computing Centre (NERSC) in Berkeley, CA under Contract No. DE-AC02-07CH11358. The high-energy X-ray experiments were performed at the 6-ID-D sector of the Advanced Photon Source, Argonne National Laboratory, under Grant No. DE-AC02-06CH11357.

Author contributions

G.Q.Y., S.Y.W., M.J.K. and C.Z.W. designed research; G.Q.Y. and S.Y.W. carried out all the simulation and data analysis; Y.Z., Y.S., B.S., F.D., Z.Y.W., R.J.Z., Y.X.Z., K.M.H. and L.Y.C. discussed and interpreted the results; M.J.K. made the experiment, and G.Q.Y., S.Y.W., and C.Z.W. co-wrote the paper.

Additional information

Supplementary information accompanies this paper at http://www.nature.com/scientificreports

Competing financial interests: The authors declare no competing financial interests.

How to cite this article: Yue, G.Q. *et al.* Local structure order in $Pd_{78}Cu_6Si_{16}$ liquid. *Sci. Rep.* **5**, 8277; DOI:10.1038/srep08277 (2015).